ORGANISMAL BIOLOGY

A new case of kleptoplasty in animals: Marine flatworms steal functional plastids from diatoms

Niels W. L. Van Steenkiste[1,2]*†, India Stephenson[1]*, María Herranz[1,2], Filip Husnik[2], Patrick J. Keeling[2], Brian S. Leander[1,2]†

To date, sea slugs have been considered the only animals known to sequester functional algal plastids into their own cells, via a process called "kleptoplasty." We report here, however, that endosymbionts in the marine flatworms *Baicalellia solaris* and *Pogaina paranygulgus* are isolated plastids stolen from diatoms. Ultrastructural data show that kleptoplasts are located within flatworm cells, while algal nuclei and other organelles are absent. Transcriptomic analysis and *rbcL* amplicons confirm the absence of algal nuclear mRNA and reveal that the plastids originate from different species of diatoms. Laboratory experiments demonstrated photosynthetic activity and short-term retention of kleptoplasts in starved worms. This lineage of flatworms represents the first known case of functional kleptoplasty involving diatoms and only the second known case of kleptoplasty across the entire tree of animals.

INTRODUCTION

Several groups of animals, including cnidarians, mollusks, chordates, sponges, acoelomorphs, and flatworms, harbor single-celled algal endosymbionts, which provide their host with carbon and oxygen derived from photosynthesis (*1–3*). Sacoglossan sea slugs offer a unique variation on this habit; they feed on algae, sequester only the algal plastids, store them in the cells that line their digestive systems, and digest the remainder of the prey (*4*). This process of stealing plastids from prey cells is called "kleptoplasty" and is better known in several lineages of single-celled eukaryotes, such as foraminiferans, dinoflagellates, and ciliates (*2*, *5*). Despite the lack of nuclear genes encoding proteins involved in photosynthesis, kleptoplasts can remain functional for as long as 10 months in the sea slug *Elysia chlorotica* (*4*, *6*). Lateral gene transfer from the algal nucleus to the animal nucleus has been proposed as a mechanism to explain plastid longevity (*7–11*), but thorough analyses of sea slug transcriptomes and genome data have not found support for this hypothesis (*12*, *13*). Long-term plastid retention is now thought to be the result of the robustness of the plastids themselves, the stability of their essential proteins, and physiological adaptations of the host (*14*).

In flatworms, endosymbiotic algae have been reported only in microturbellarians called "rhabdocoels." Several freshwater species harbor *Chlorella* (*15*), while some marine species of *Baicalellia* (1 of 23 species) and *Pogaina* (all 17 species) have algal endosymbionts of unknown origin. Initially described as "zooxanthellae" (*16*), the endosymbionts of these marine rhabdocoels occur subepidermally in the mesenchyme and between the atrial organs (*17*, *18*). Even before kleptoplasty was demonstrated in sacoglossan sea slugs (*19*), it was noticed that these flatworm endosymbionts appear to lack algal nuclei (*20*). This observation suggests that kleptoplasty in metazoans might not be limited to sacoglossans. However, the origin and characteristics of this endosymbiotic association in marine rhabdocoels remain unclear. This poor state of knowledge is not unexpected because it reflects the fact that microscopic animals, so-called meiofauna, are a neglected component of most marine biodiversity surveys (*21*).

To investigate this endosymbiotic association in uncultured marine flatworms, we used a combination of high-resolution microscopy and molecular phylogenetic analyses on specimens of *Baicalellia solaris* and *Pogaina paranygulgus* (*22*). Single-animal transcriptomics and photosynthesis and starvation experiments on *B. solaris* further support and elucidate this kleptoplastic association. This study presents the first case of functional kleptoplasty in flatworms and only the second example across the entire tree of animals.

RESULTS

Anatomical position and ultrastructure of the plastids

Light microscopy (LM), confocal laser scanning microscopy (CLSM), and transmission electron microscopy (TEM) demonstrated the ultrastructure and anatomical position of the sequestered plastids and confirmed the absence of algal nuclei in the host tissues. Golden-brown plastids were distributed in the mesenchyme and between the atrial organs of the worms (Figs. 1, A and B, and 2, A and B). Frustules of pennate diatoms were present within the gut of several flatworms (Fig. 1B and figs. S1, C and D, and S2F). The plastids showed strong chlorophyll autofluorescence in the red spectrum (Figs. 1C and 2C and fig. S3, D to I). Degraded plastids with a dark brown to black appearance (Figs. 1, A and B, and 2B) showed no autofluorescence (Fig. 2C). Plastids are more concentrated below the epidermis and on the dorsal side of the animals (fig. S3). The number and density of plastids varied among individual worms; a few freshly collected specimens of *B. solaris* (fig. S1, A and B) contained no plastids at all. Variations in plastid size were smaller within and between individuals of *B. solaris* (5 to 20 μm; Fig. 1B and fig. S1C) than within and between individuals of *P. paranygulgus* (5 to 45 μm; fig. S2, A and B).

Individual and small groups of plastids were stored intracellularly and were closely associated with host nuclei, host mitochondria with flat (lamellar) cristae, and host lipid droplets [Figs. 1(D and E) and 2 (D and E) and fig. S4]. The ultrastructure of the plastid was typical of secondary plastids of heterokonts with triple-stacked thylakoids, few anastomoses, and a peripheral three-thylakoid girdle lamella (Fig. 1E). The plastids also contained a few small lipid droplets
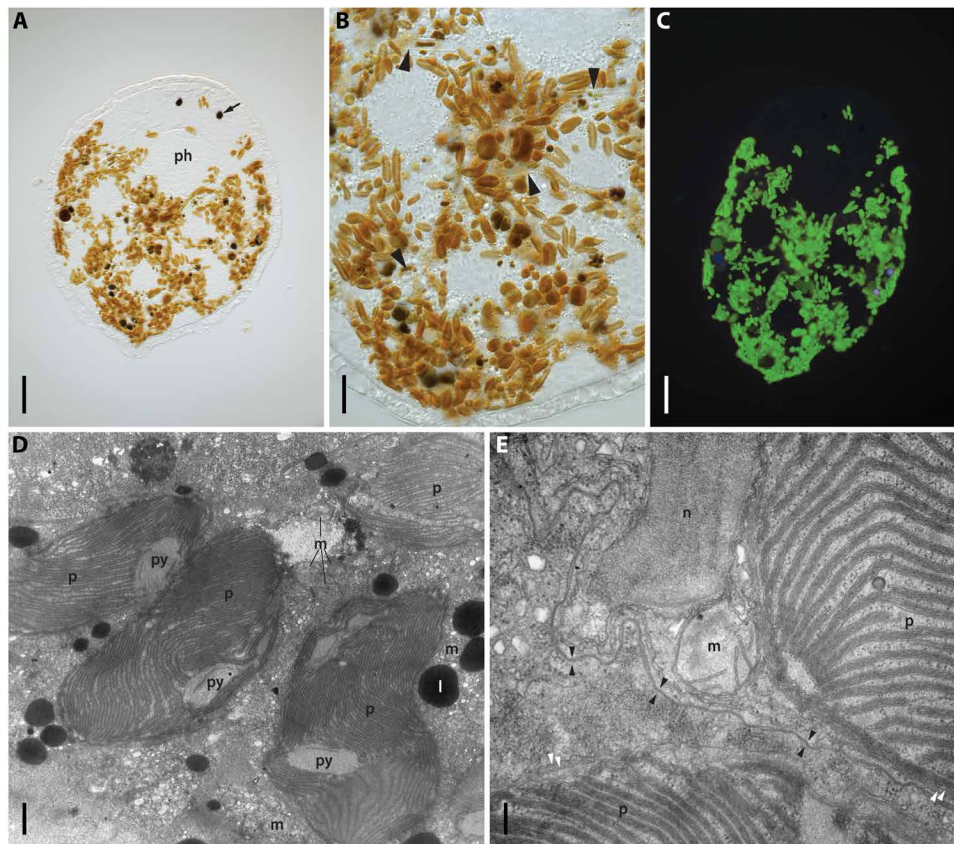
Fig. 1. Light, fluorescence, and transmission electron micrographs of *B. solaris* and its kleptoplasts. (**A**) Live specimen with eyes (arrow), pharynx, and golden-brown kleptoplasts; darker plastids are being degraded. (**B**) Kleptoplasts and empty frustules of pennate diatoms (large black arrowheads). (**C**) Autofluorescence of kleptoplasts densely packed under the epidermis and within the mesenchyme. (**D**) Heterokont kleptoplasts in host cells. (**E**) Cell junction (small black arrowheads) between two host cells, each containing a heterokont kleptoplast surrounded by at least two membranes (small white arrowheads). l, lipid vesicle; m, mitochondria; n, nucleus; p, plastid; ph, pharynx; py, pyrenoid. Scale bars, 50 (A), 20 (B), 50 (C), and 1 μm (D) and 200 nm (E).

and an elongate, oval, or spindle-shaped pyrenoid crossed by a thylakoid lamella [Figs. 1 (D and E) and 2 (D and E) and fig. S4]. Two membranes appear to surround the plastids (Fig. 1E and fig. S4D). We did not observe dividing plastids, whole algal cells, or other algal organelles within the mesenchyme.

Transcriptomics and phylogenetic analysis of plastid genes
Plastid gene sequences generated from polymerase chain reaction (PCR) and transcriptomics of *B. solaris* demonstrated the origin of the plastids and the absence of expressed nuclear-encoded diatom protein genes. While most transcripts are of flatworm origin, diatom sequences constitute the largest fraction of nonmetazoan eukaryotic transcripts (fig. S5). Annotated *B. solaris* transcripts of five plastid-encoded genes, photosystem II protein D1 (*psbA*), photosystem II CP47 protein (*psbB*), adenosine 5′-triphosphate synthase subunit alpha (*atpA*), photosystem I P700 apoprotein A2 (*psaB*), and ribulose bisphosphate carboxylase large chain (*rbcL*), were almost exclusively of diatom origin (data file S1). These genes grouped together with diatom and diatom-derived plastid genes in molecular phylogenetic analyses of a concatenated dataset (Fig. 3). In four of five individual gene phylogenies, *B. solaris* transcripts are closely related to the respective plastid genes of diatoms and close relatives (figs. S6 to S10). Poly(A) enrichment was used to specifically test for the presence of polyadenylated nuclear diatom genes,

but all annotated *B. solaris* protein transcripts of diatom origin were exclusively plastid-encoded (data file S2). These plastid-encoded transcripts are not polyadenylated and only captured when containing AT-rich regions. An *rbcL* gene tree, including sequences from representative diatoms, transcripts from the *B. solaris* transcriptome, and PCR-amplified sequences from additional *B. solaris* and *P. paranygulgus* specimens, demonstrated that *B. solaris* and *P. paranygulgus* can sequester plastids from different species of pennate diatoms (fig. S11).

Photosynthetic activity and plastid retention
Oxygen consumption measurements and photosynthesis inhibition experiments on starved individuals of *B. solaris* in a laboratory setting show that kleptoplasts maintain photosynthesis and are retained for more than a week. Three replicates of 25 pooled *B. solaris* individuals display a light-dependent oxygen evolution and a decline in oxygen saturation in the dark, allowing a calculation of mean gross photosynthesis. The magnitude of photosynthetic activity in 7-day starved specimens was similar to a dense culture of the chlorophyte alga *Tetraselmis tetrathele* (Fig. 4A). After 1 week of starvation, plastid retention rates were higher in untreated *B. solaris* specimens compared to those treated with the photosynthesis inhibitor monolinuron (Fig. 4B). We also observed lower densities of plastids in worms treated with the highest concentration
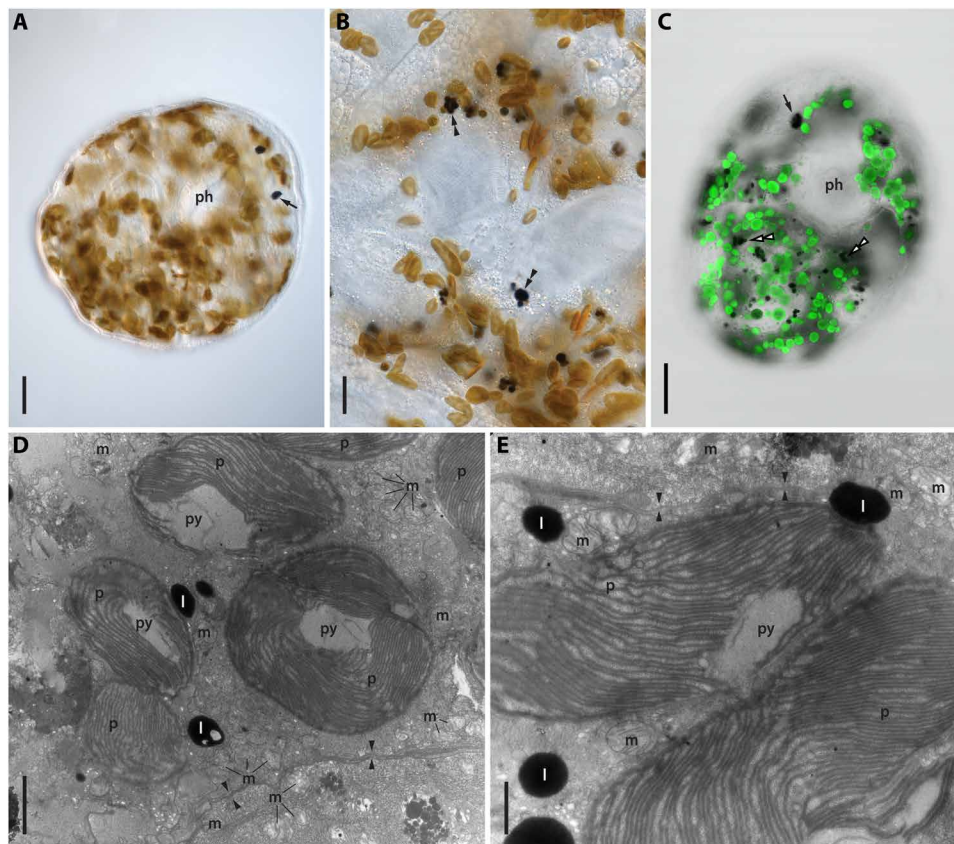
Fig. 2. Light, confocal, and transmission electron micrographs of *P. paranygulgus* and its kleptoplasts. (**A**) Live specimen with eyes (arrow), pharynx, and golden-brown kleptoplasts. (**B**) Intact (golden brown) and degraded (double black arrowheads) kleptoplasts. (**C**) Autofluorescence of kleptoplasts in a juvenile specimen; degraded plastids (double white arrowheads) show no autofluorescence. (**D** and **E**) Heterokont kleptoplasts adjacent to flatworm mitochondria, lipid droplets and cell junction (arrowheads). Scale bars, 50 (A), 20 (B), 50 (C), 2 (D), and 1 μm (E).

of monolinuron than in the other two treatment groups (fig. S12). All worms lost their kleptoplasts after 2 weeks of starvation.

DISCUSSION

Before this study, known examples of kleptoplasty in animals were restricted only to sacoglossan sea slugs. Symbiotic interactions of meiofaunal animals with other organisms are poorly understood, and earlier reports of putative algal endosymbionts in marine rhabdocoels, such as *Pogaina*, are limited to LM (*17*, *20*) and a few anecdotal TEM observations (*18*). On the basis of the occurrence of diatoms in the gut, endosymbioses in marine rhabdocoels were inferred to be similar to the endosymbiosis between the diatom *Licmophora* and the acoel *Convoluta convoluta* (*23*); however, in the latter case, the entire diatom prey cell is sequestered and maintained (*24*). Therefore, our data demonstrate that the endosymbionts in the rhabdocoels *B. solaris* and *P. paranygulgus* are fundamentally different from those in the acoel *Convoluta*, because they are individual plastids stolen from diatom prey cells, i.e., kleptoplasts, rather than whole diatom prey cells. All annotated protein transcripts from *B. solaris* of diatom origin were exclusively plastid-encoded, which is the expected result for kleptoplasts.

The molecular data showing that the kleptoplasts in *B. solaris* and *P. paranygulgus* were derived from pennate diatoms are consistent with microscopy observations of empty pennate diatom frustules in the gut of live specimens and the ultrastructure of the sequestered plastids. Although diatom plastids have four enveloping membranes (*25*), only two or possibly three membranes surround the kleptoplasts in *B. solaris*. The outermost plastid membrane, which is continuous with the rough endoplasmic reticulum and the nuclear envelope of the intact diatom, is presumably left behind during the process of plastid isolation. Many rhabdocoels are known to feed on diatoms (*26*); *B. solaris* and *P. paranygulgus* ingest live diatoms, somehow open the frustules, sequester the plastids, and digest the remainder of the prey cell. The flatworms can sequester plastids from different but closely related species of pennate diatoms. More research is required to determine prey cell specificity and how species affinities of flatworm plastids potentially correlate with seasonal variation in diatom species composition and abundance. One hypothesis is that kleptoplasts might serve as a prolonged carbon source following the collapse of diatom blooms.

To determine the mechanisms behind plastid uptake, sequestration, longevity, and carbon fixation and exchange in marine rhabdocoels, we need a better understanding of rhabdocoel biology. While sequestration of whole algal cells by flatworms is restricted to freshwater rhabdocoels, other exogenous organelles, such as the nematocysts from cnidarian prey, can be stolen and incorporated into the tissues of other lineages of turbellarians. In these cases, amoeboid phagocytes originating in the gastrodermis transport nematocysts through
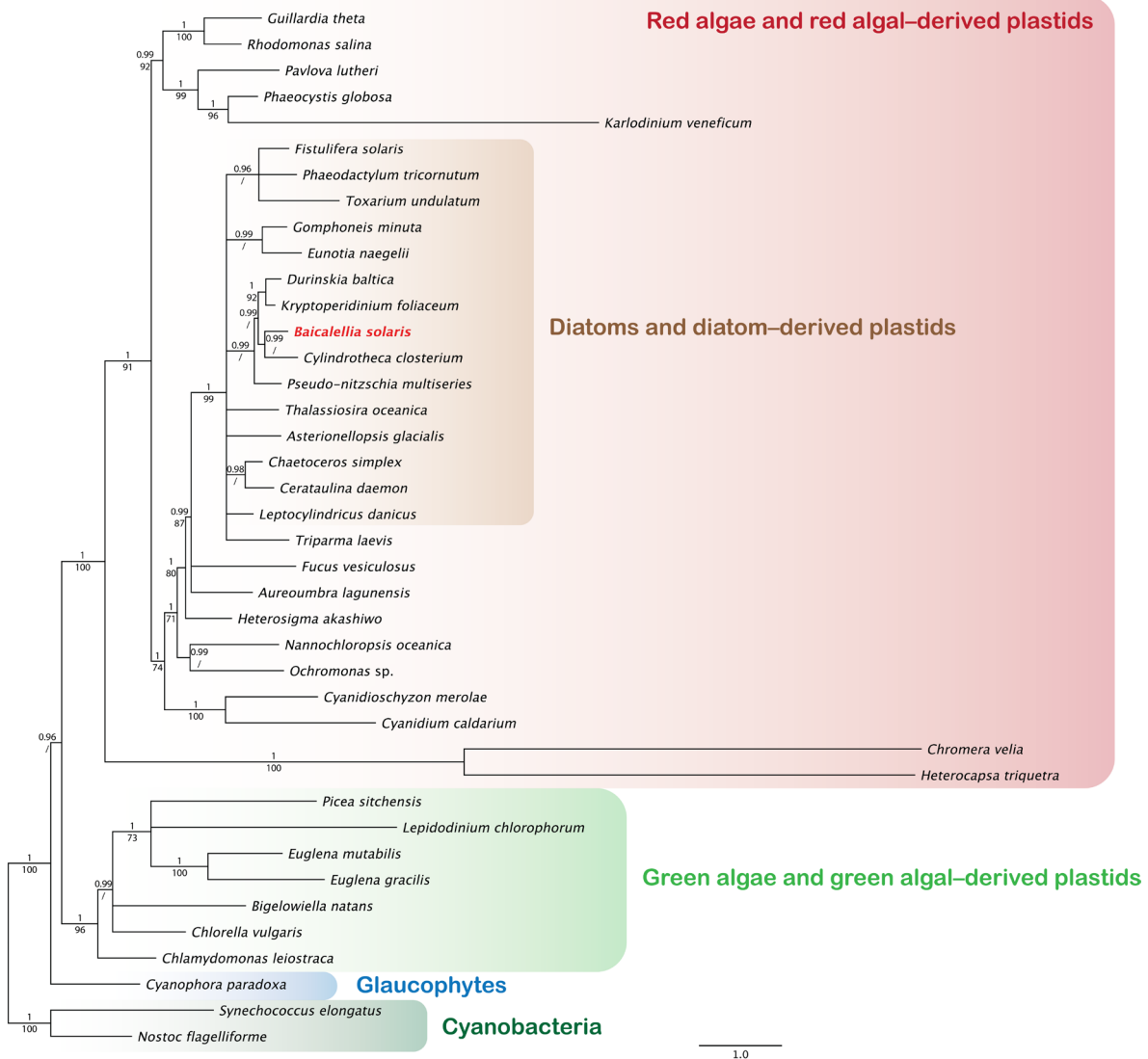
Fig. 3. A phylogeny of five partial plastid genes based on transcripts from the transcriptome of *B. solaris* demonstrates that its kleptoplasts are of diatom origin. A concatenated 2956–base pair alignment of *psaB*, *psbA*, *psbB*, *atpA*, and *rbcL* was run in MrBayes v3.2.6. Support was assessed with Bayesian posterior probabilities (pp, above branches) and maximum likelihood bootstrap replicates (bs, below branches) from a RAxML analysis. Unsupported branches are collapsed (pp < 0.95) or indicated with a "/" when not supported in RAxML. Scale bar, substitutions/site.

the mesenchyme and into the epidermis (*27*). It is possible that a similar mechanism is involved in kleptoplasty; however, how certain organelles are selectively targeted for sequestration, and thus evade digestion, remains unclear.

Our experimental data suggest that kleptoplasts in *B. solaris* still had functional photosystems after a week of starvation; the magnitude of photosynthetic activity in 7-day starved specimens was similar to a culture of chlorophyte algae. The rapid loss of plastids during the second week of starvation shows that plastids are only retained for a short time. The inhibition of photosynthesis with monolinuron indicates that a disturbed photophysiology negatively affects plastid stability in the worms but did not influence survival rates of the animals in the short term. Long-term starvation experiments with photosynthesis inhibitors could answer the question whether the plastids provide the host with a fitness advantage by supplying fixed carbon during the first 2 weeks of starvation. Combined with carbon-tracing experiments, these starvation experiments could determine whether carbon is acquired through the exchange of photosynthate from photosynthesizing plastids or whether kleptoplasts are instead kept as passive food storage, whereby carbon is released only after plastid degradation (*28*, *29*). The digestion of kleptoplast membranes would provide the host with a lipid-rich food source and might explain the abundance of lipid droplets near kleptoplasts within host cells. Some specimens of *B. solaris* and *P. paranygulgus* had very few kleptoplasts, suggesting that the plastids provide a facultative carbon source for these species.

Among sacoglossans, functional kleptoplasty varies in the amount of time kleptoplasts are retained. Long-term retention species maintain plastids with functional photosystems for several months, while short-term retention species can only keep functional plastids for up to 2 weeks (*4*). Long-term and short-term functional kleptoplasty have evolved multiple times independently within Sacoglossa (*30*). There is phylogenetic evidence that this is also the case for rhabdocoel flatworms.
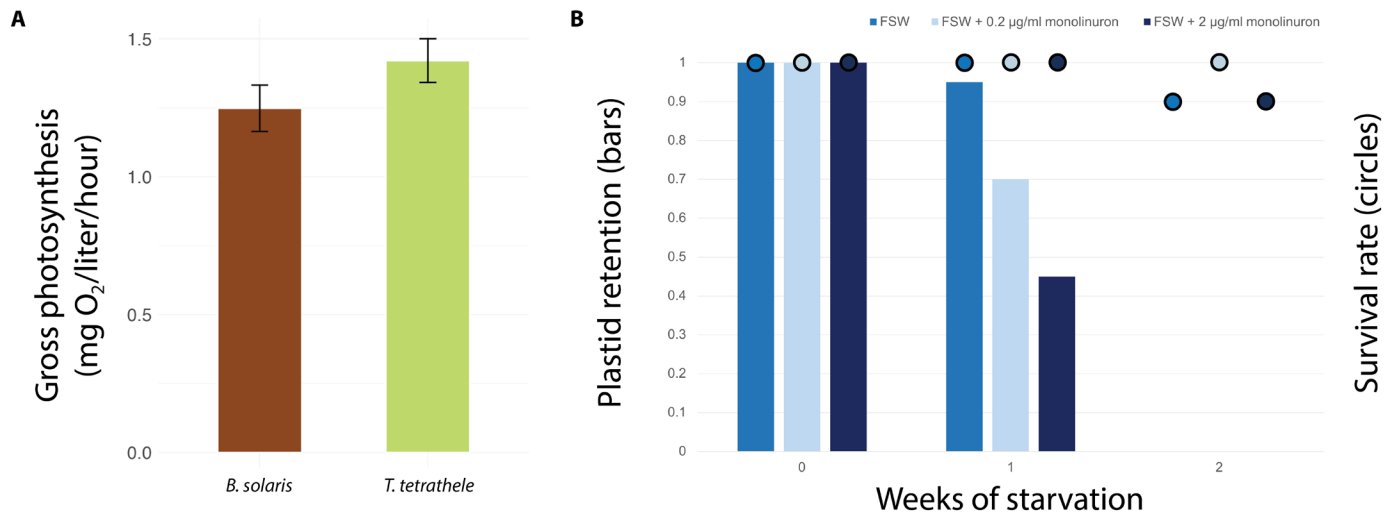
Fig. 4. Functional kleptoplasty and short-term retention of plastids in *B. solaris* is shown by photosynthetic activity and the loss of plastids in starved specimens over time. (**A**) Photosynthetic activity in *B. solaris* specimens starved for 7 days (*n* = 25) compared with the chlorophytic alga *T. tetrathele* (~500,000 cells/ml). Gross photosynthesis was calculated by summing the net photosynthesis and respiration rates. Data represent means ± SE. (**B**) Plastid retention (proportion of kleptoplastic individuals) and survival rate (proportion of surviving individuals) in filtered seawater (*n* = 20) and under differential treatments with the photosynthesis inhibitor monolinuron (*n* = 20 in each treatment). FSW, filtered seawater.

Baicalellia and *Pogaina* are closely related but are not sister taxa, and *B. solaris* is the only kleptoplastic species of *Baicalellia*, deeply nested within the genus (*22*). Although *B. solaris* seems to be a short-term retention species, we do not know whether kleptoplasts in species of *Pogaina* are photosynthetically active and how long they are retained. Additional experiments with *B. solaris* and species of *Pogaina* will help determine the mechanisms behind plastid uptake, sequestration, longevity, and carbon fixation and exchange; these experiments would be greatly facilitated by establishing viable laboratory cultures of kleptoplast-bearing rhabdocoels and the diatoms from which they sequester plastids. Although some of these species can constitute an abundant component of the meiofauna associated with intertidal macroalgae, marine rhabdocoels have never been cultured; their behavior and interactions with other species remain poorly understood. Nonetheless, by using a diverse array of culture-independent research approaches, this study has demonstrated the first known case of functional kleptoplasty involving diatoms and only the second known case of kleptoplasty in animals, indicating that an improved understanding of microscopic animals, such as rhabdocoels, will provide deeper insights into the prevalence and influence of endosymbioses in evolutionary history.

MATERIALS AND METHODS
Sample collection and imaging of live animals
Specimens of *B. solaris* were collected between 2016 and 2018 from macroalgae in the rocky intertidal at Clover Point, Victoria, BC (48°24′12″N, 123°21′03″W) and West Beach, Calvert Island, BC (51°39′07″N, 128°08′33″W). Specimens of *P. paranygulgus* were collected in 2015, 2016, and 2018 from intertidal mudflats at Mud Bay Park, Surrey, BC (49°05′09″N, 122°51′39″W) and Ladysmith Inlet, Nanaimo, BC (49°01′28″N, 123°50′59″W). Live worms were isolated using the $MgCl_2$ decantation method and the oxygen depletion method (*31*), mounted in seawater, and photographed using a ZEISS Axioplan 2 microscope equipped with differential interference contrast (DIC)

optics and a ZEISS Axiocam 503 color camera. Live specimens were imaged using an Olympus FV1000 Multiphoton confocal laser scanning microscope (Olympus, Tokyo, Japan) at the University of British Columbia (UBC) Bioimaging Facility. Optical sections were taken from specimens excited at 635 nm (emission range, 650 to 750 nm). Optical sections and z-stack projection micrographs were compiled with Fiji version 2.00 (Wayne Rasband, National Institutes of Health).

Specimens of *B. solaris* and *P. paranygulgus* were used for TEM, genomic DNA extraction, and amplicon sequencing. The limited availability of *P. paranygulgus* prevented us from using specimens of this species for RNA sequencing (RNA-seq), as well as photosynthesis and starvation experiments.

Transmission electron microscopy
Isolated specimens were pipetted onto a coverslip coated with poly-L-lysine and fixed with 2.5% (v/v) glutaraldehyde in filtered seawater for 1 hour. Glutaraldehyde was drawn off using a pipette, and specimens were post-fixed in 1% (w/v) osmium tetroxide with filtered seawater at 4°C for 1 hour. Specimens were rinsed with seawater and stuck to the coverslip using a large drop of low–melting point agar and then dehydrated through a graded ethanol series (30, 50, 75, 85, 90, 95, and 100%) at 10 min each. Specimens were washed in 1:1 ethanol:acetone for 10 min and 100% acetone for 10 min. After infiltration with a 1:1 acetone-resin mixture for 10 min, specimens were embedded in EPON 812 Resin for 12 hours, after which the resin was polymerized at 65°C for 24 hours.

Specimens were cut from the resin using a fine razor and glued to a resin stub in the desired orientation for sectioning. Ultrathin (45 nm) sections were cut using a DiATOME Ultracut diamond knife mounted on a Leica Ultracut E Ultramicrotome. Sections were placed on Formvar-coated copper grids and triple-stained with lead citrate for 10 min, uranyl acetate for 5 min, followed by lead citrate for 10 min. Stained grids were viewed under a Hitachi H7600 TEM with an accelerating voltage of 80 kV and photographed with an AMT XR50 CCD camera.

Genomic DNA extraction and amplicon sequencing

Genomic DNA was extracted from entire specimens of *B. solaris* and *P. paranygulgus* using the DNeasy Blood & Tissue Kit (QIAGEN), following the manufacturer's instructions. An 862–base pair (bp) region of the plastid *rbcL* gene, which encodes for the large subunit of the ribulose-1,5-biphosphate carboxylase/oxygenase, was PCR-amplified using Illustra PuReTaq Ready-To-Go PCR beads (GE Healthcare), and the primers and thermocycling conditions listed in table S1. Amplicons were visualized on 1.5% agarose gels stained with GelRed (Biotium) and enzymatically cleaned before sequencing with Illustra ExoProStar S (GE Healthcare). Clean amplicons were sequenced in 10 μl containing 1 μl of BigDye Terminator (BDT) v3.1 (Applied Biosystems), 2 μl of BDT buffer, 0.5 μM amplification primer, and 1 to 2 μl of PCR product. Cleaned sequencing products were run on an Applied Biosystems 3730S 48-capillary DNA analyzer by the Nucleic Acid Protein Service Unit at UBC. Resulting clean trace files were assembled into full sequences in Geneious v9.1.5 (*32*) and subjected to a BLAST (Basic Local Alignment Search Tool) search on the National Center for Biotechnology Information (NCBI) website (www.ncbi. nlm.nih.gov) and an identification request in the Public Record Barcode Database on the BOLD (Barcode Of Life Data) website (www. boldsystems.org/index.php/) to verify the plastid's taxonomic origin.

RNA extraction, RNA-seq library preparation, and sequencing

Total RNA extraction and preparation of a full-length polyA-selected complementary DNA and sequencing library from a single specimen of *B. solaris* were done using the reagents and following the protocol in the Smart-seq2 pipeline (*33*). The specimen was starved for a week to avoid contamination with freshly ingested prey cells. Library quantity and quality were measured using a 2100 Bioanalyzer (Agilent) before sequencing. Paired-end sequencing was performed on an Illumina HiSeq 2500. The library was barcoded on one-fourth of a flow cell and sequenced with 125-bp paired-end reads (high-output mode).

Transcriptome data analysis

The quality of the raw RNA-seq data was assessed with FastQC v0.11.5. Paired-end reads were subsequently trimmed and de novo assembled into transcripts with Trinity v2.4.0 (*34, 35*). Post-assembly quality control and taxonomic partitioning were done with BlobTools (*36, 37*) and phyloFlash (*38*). We did not find any substantial contamination. Transcript abundance was estimated with the RSEM (RNA-Seq by Expectation Maximization) method using the normalized expression values TPM (transcripts per kilobase million) and FPKM (fragments per kilobase million). Candidate coding regions were identified with TransDecoder v5.1.0. Completeness of the transcriptome was assessed with BUSCO v3.0.2b (*39, 40*) and compared to other available flatworm transcriptomes (fig. S13) (*41*). The transcriptome was annotated using the Trinotate v3.1.1 annotation pipeline (*42*), which includes blastx and blastp homology searches to the BLAST+/SwissProt databases (data files S1 and S2), protein domain identification with HMMER/Pfam, signal peptide and transmembrane domain prediction with signalP/tmHMM, and functional annotation against eggNOG/GO/KEGG databases.

Molecular phylogenetic analyses

Sequences of five plastid genes, *psaB*, *psbA*, *psbB*, *atpA*, and *rbcL*, from the transcriptome of *B. solaris* were aligned with a selected dataset of other eukaryotic sequences using the E-INSI algorithm in MAFFT (Multiple Alignment using Fast Fourier Transform) (*43*). In addition, *rbcL* sequences of the kleptoplasts from *B. solaris* and *P. paranygulgus* and a representative set of diatoms were also aligned. The alignments were trimmed and translated into amino acids to check for inconsistencies and remove large gaps in Geneious. A concatenated dataset was created from the five eukaryote alignments.

Best-fit partitioning schemes and models of molecular evolution (table S2) were recovered in PartitionFinder v1.1.0 based on a greedy search with PhyML and the Akaike information criterion (*44*). These partitions and models of evolution were subsequently used in the RAxML v8.2.11 maximum likelihood analyses (*45*) and MrBayes v3.2.6 Bayesian analyses (*46*) on the concatenated dataset and separate gene datasets, respectively. RAxML was run in Geneious, performing a best-scoring tree search and nonparametric bootstrapping (1000 pseudoreplicates). Bayesian analyses were run on XSEDE in the CIPRES Science Gateway (www.phylo.org), using default prior and MCMC settings, in two independent simultaneous runs for 100 million generations. Trees were sampled every 1000th generation after a 25% burnin. Convergence was determined on the basis of the logL values and the average deviation of split frequencies. For each Bayesian analysis, the resulting 75,000 trees were summarized in a 50% majority-rule consensus tree. We considered a 70% bootstrap and 0.95 posterior probabilities as threshold values for branch support (*47*).

Starvation experiments

Sixty freshly collected *B. solaris* specimens were divided randomly into three different treatments using filtered seawater from the worm's collection site: (i) 20 worms in filtered seawater, (ii) 20 worms in filtered seawater with 0.2 μg of 3-(4-chlorophenyl)-1-methoxy-1-methylurea (monolinuron) ml^{-1} added, (iii) 20 worms in filtered seawater with 2 μg of monolinuron ml^{-1} added. Individual worms were kept separately in 12-well culture plates with each well containing 2.5 ml of medium. All treatments were incubated at 12°C and illuminated at 65 μmol quanta m^{-2} s^{-1} under a 12-hour light/12-hour dark cycle for 2 weeks. Filtered seawater was refreshed daily. Worms were counted every day, and plastid retention was evaluated every week with the aid of a ZEISS Stemi 508 stereo microscope and a ZEISS Axiovert 200 inverted microscope equipped with a ZEISS Axiocam 503 color camera. Survival rates and plastid retention rates were calculated and visualized using Microsoft Excel.

Analysis of photosynthetic activity

Oxygen consumption measurements were undertaken to estimate photosynthetic rates. Oxygen saturation (O$_2$ mg/liter) was measured using an SDR SensorDish Reader (PreSens, Regensburg, Germany) with light-emitting diode lights for noninvasive optical fluorescence oxygen sensing and a sealed 24-chamber glass microplate with 0.2-ml wells (Loligo Systems, Copenhagen, Denmark). Individuals of *B. solaris* were starved in sterile seawater and incubated at 16°C on a 14-hour light/10-hour dark cycle for 7 days and acclimatized to room temperature for 3 hours before the experiments.

Three wells each contained 25 worms in sterile seawater medium. The number of replicates was limited by the number of specimens available, as *B. solaris* is not culturable and specimens need to be collected in the field. A positive control consisted of three replicate wells containing a culture of the marine chlorophyte *T. tetrathele* (~500,000 cells/ml). Three replicate wells with sterile seawater were used as a negative control. Remaining wells contained deionized water.

Wells were overfilled, checked for air bubbles, and then sealed with transparent PCR film (Thermo Fisher Scientific, Waltham, MA, USA). The microplate was placed on the SDR reader and incubated in the dark for a 10-min acclimatization period before illumination. A 90-min light treatment in light-saturated conditions (light intensity, 120 μmol quanta m^{-2} s^{-1}) was provided by a NanoTech T5 Reflector light (SunBlaster, Langley, Canada), followed by a 90-min dark treatment in which an opaque black box was placed over the wells. Oxygen measurements were made every 15 s during the treatments. The experiment was conducted at room temperature, with the microplate placed in a water bath to maintain constant temperature. Specimens were observed at the end of the experiment to check whether they were still alive.

For analysis, 20-min optimal measurement intervals were chosen from each 90-min measurement period based on having the least temperature fluctuation (with temperature ranges of 0.05°C and 0.04°C for light and dark treatments, respectively) to eliminate any confounding effect of temperature on oxygen saturation. The rate of change of oxygen saturation (O_2 mg/liter per hour) over the treatment intervals was calculated for each replicate using a linear regression. The average of the negative control slopes was subtracted from the experimental wells to correct for background microbial respiration. Gross photosynthesis for each replicate was estimated as gross photosynthetic rate = net photosynthesis (oxygen evolution) + respiration. Mean and SE were calculated and visualized on a bar plot. All data analyses were conducted in RStudio v1.0.143 (RStudio Inc., Boston, MA, USA).

SUPPLEMENTARY MATERIALS

Supplementary material for this article is available at http://advances.sciencemag.org/cgi/content/full/5/7/eaaw4337/DC1

Fig. S1. Freshly collected specimens of *B. solaris*.
Fig. S2. Freshly collected specimens of *P. paranygulgus*.
Fig. S3. LM and CLSM micrographs of *P. paranygulgus*.
Fig. S4. TEM micrographs of *B. solaris*.
Fig. S5. Taxonomic partitioning of the transcriptome of *B. solaris* with BlobTools.
Fig. S6. Bayesian majority-rule consensus tree of the partial *psbA* gene recovered from the transcriptome of *B. solaris*.
Fig. S7. Bayesian majority-rule consensus tree of the partial *psbB* gene recovered from the transcriptome of *B. solaris*.
Fig. S8. Bayesian majority-rule consensus tree of the partial *psaB* gene recovered from the transcriptome of *B. solaris*.
Fig. S9. Bayesian majority-rule consensus tree of the partial *atpA* gene recovered from the transcriptome of *B. solaris*.
Fig. S10. Bayesian majority-rule consensus tree of the partial *rbcL* gene recovered from the transcriptome of *B. solaris*.
Fig. S11. Bayesian majority-rule consensus tree based on an alignment of *rbcL* sequences of representative pennate diatoms, PCR-amplified *rbcL* sequences from the kleptoplasts of different specimens of *B. solaris* and *P. paranygulgus*, and *rbcL* transcripts recovered from the transcriptome of *B. solaris*.
Fig. S12. Loss of kleptoplasts in three specimens of *B. solaris* during the starvation experiment.
Fig. S13. Busco assessment results of the assembled transcriptome of *B. solaris* and other publicly available flatworm transcriptomes.
Table S1. Amplification primers and thermocycling conditions for the partial *rbcL* gene.
Table S2. Best-fit partitioning schemes and models of molecular evolution for five plastid genes and the concatenated alignment recovered in PartitionFinder v1.1.0.
Movie S1. Live adult specimen of *B. solaris* full of kleptoplasts squeezed under a cover slip.
Movie S2. Live adult specimen of *B. solaris* full of kleptoplasts squeezed under a cover slip.
Movie S3. Compilation of CLSM micrographs showing the autofluorescence of the kleptoplasts in a live juvenile specimen of *P. paranygulgus*.
Data file S1. Blastp and blastx annotated transcripts of the plastid-encoded genes, *psbA*, *psbB*, *atpA*, *psaB*, and *rbcL*, in the transcriptome of *B. solaris* are almost exclusively of diatom origin.
Data file S2. Blastp and blastx annotated transcripts of diatom origin in the transcriptome of *B. solaris* are all plastid-encoded.
References (*48*–*49*)

REFERENCES AND NOTES

1. A. A. Venn, J. E. Loram, A. E. Douglas, Photosynthetic symbioses in animals. *J. Exp. Bot.* **59**, 1069–1080 (2008).
2. M. D. Johnson, The acquisition of phototrophy: Adaptive strategies of hosting endosymbionts and organelles. *Photosynth. Res.* **107**, 117–132 (2011).
3. J. Melo Clavijo, A. Donath, J. Serôdio, G. Christa, Polymorphic adaptations in metazoans to establish and maintain photosymbioses. *Biol. Rev. Camb. Philos. Soc.* **93**, 2006–2020 (2018).
4. K. Händeler, Y. P. Grzymbowski, P. J. Krug, H. Wägele, Functional chloroplasts in metazoan cells—A unique evolutionary strategy in animal life. *Front. Zool.* **6**, 28 (2009).
5. D. K. Stoecker, M. D. Johnson, C. de Vargas, F. Not, Acquired phototrophy in aquatic protists. *Aquat. Microb. Ecol.* **57**, 279–310 (2009).
6. B. J. Green, W.-Y. Li, J. R. Manhart, T. C. Fox, E. J. Summer, R. A. Kennedy, S. K. Pierce, M. E. Rumpho, Mollusc-algal chloroplast endosymbiosis. Photosynthesis, thylakoid protein maintenance, and chloroplast gene expression continue for many months in the absence of the algal nucleus. *Plant Physiol.* **124**, 331–342 (2000).
7. S. K. Pierce, N. E. Curtis, J. J. Hanten, S. L. Boerner, J. A. Schwartz, Transfer, integration and expression of functional nuclear genes between multicellular species. *Symbiosis* **43**, 57–64 (2007).
8. S. K. Pierce, X. Fang, J. A. Schwartz, X. Jiang, W. Zhao, N. E. Curtis, K. M. Kocot, B. Yang, J. Wang, Transcriptomic evidence for the expression of horizontally transferred algal nuclear genes in the photosynthetic sea slug, *Elysia chlorotica. Mol. Biol. Evol.* **29**, 1545–1556 (2012).
9. M. E. Rumpho, J. M. Worful, J. Lee, K. Kannan, M. S. Tyler, D. Bhattacharya, A. Moustafa, J. R. Manhart, Horizontal gene transfer of the algal nuclear gene *psbO* to the photosynthetic sea slug *Elysia chlorotica. Proc. Natl. Acad. Sci. U.S.A.* **105**, 17867–17871 (2008).
10. J. A. Schwartz, N. E. Curtis, S. K. Pierce, Using algal transcriptome sequences to identify transferred genes in the sea slug, *Elysia chlorotica. Evol. Biol.* **37**, 29–37 (2010).
11. J. A. Schwartz, N. E. Curtis, S. K. Pierce, FISH labeling reveals a horizontally transferred algal (*Vaucheria litorea*) nuclear gene on a sea slug (*Elysia chlorotica*) chromosome. *Biol. Bull.* **227**, 300–312 (2014).
12. C. Rauch, J. de Vries, S. Rommel, L. E. Rose, C. Woehle, G. Christa, E. M. Laetz, H. Wägele, A. G. M. Tielens, J. Nickelsen, T. Schumann, P. Jahns, S. B. Gould, Why it is time to look beyond algal genes in photosynthetic slugs. *Genome Biol. Evol.* **7**, 2602–2607 (2015).
13. D. Bhattacharya, K. N. Pelletreau, D. C. Price, K. E. Sarver, M. E. Rumpho, Genome analysis of *Elysia chlorotica* egg DNA provides no evidence for horizontal gene transfer into the germ line of this kleptoplastic mollusc. *Mol. Biol. Evol.* **30**, 1843–1852 (2013).
14. J. de Vries, G. Christa, S. B. Gould, Plastid survival in the cytosol of animal cells. *Trends Plant Sci.* **19**, 347–350 (2014).
15. A. M. McCoy, I. Balzer, Algal symbiosis in flatworms, in *Symbiosis: Mechanisms and Model Systems*, J. Seckbach, Ed. (Springer Netherlands, 2001), pp. 559–574.
16. L. von Graff, Marine Turbellarien Orotavas und der Küsten Europas. Ergebnisse einiger, mit Unterstützung der kais. Akademie der Wissenschaften in Wien (aus dem Legate Wedl) in den Jahren 1902 und 1903 unternommen Studienreise. II. Rhabdocoela. *Z. Wiss. Zool.* **83**, 68–148 (1905).
17. A. Luther, Untersuchungen an Rhabdocoelen Turbellarien. VII. Über einige marine Dalyellioida. VIII. Beiträge zur Kenntnis der Typhloplanoida. *Acta Zool. Fenn.* **55**, 1–122 (1948).
18. N. A. Watson, Intrageneric variation in spermiogenesis, spermatozoa, and ocelli in *Pogaina* (Platyhelminthes, Rhabdocoela, Provorticidae). *Invertebr. Biol.* **118**, 243–257 (1999).
19. S. Kawaguti, T. Yamasu, Electron microscopy on the symbiosis between an elysioid gastropod and chloroplasts from a green alga. *Biol. J. Okayama Univ.* **11**, 57–64 (1965).
20. E. Marcus, Turbellaria Brasileiros (9). *Bol. Fac. Fil. Ci. Letras Univ. São Paulo* **16**, 5–215 (1951).
21. M. Curini-Galletti, T. Artois, V. Delogu, W. H. De Smet, D. Fontaneto, U. Jondelius, F. Leasi, A. Martínez, I. Meyer-Wachsmuth, K. S. Nilsson, P. Tongiorgi, K. Worsaae, M. A. Todaro, Patterns of diversity in soft-bodied meiofauna: Dispersal ability and body size matter. *PLOS ONE* **7**, e33801 (2012).
22. I. Stephenson, N. W. L. Van Steenkiste, B. S. Leander, Molecular phylogeny of neodalyellid flatworms (Rhabdocoela), including three new species from British Columbia. *J. Zool. Syst. Evol. Res.* **57**, 41–56 (2019).
23. P. Ax, Neue *Pogaina*-Arten (Turbellaria, Dalyelliodа) mit Zooxanthellen aus dem Mesopsammal der Nordsee- und Mittelmeerküste. *Mar. Biol.* **5**, 337–340 (1970).
24. G. Apelt, Die Symbiose zwischen dem acoelen Turbellar *Convoluta convoluta* und Diatomeen der Gattung *Licmophora. Mar. Biol.* **3**, 165–187 (1969).
25. F. E. Round, R. M. Crawford, D. G. Mann, *The Diatoms: Biology and Morphology of the Genera* (Cambridge Univ. Press, 1990).
26. A. Luther, Die turbellarien ostfennoskandiens. III. Neorhabdocoela 1. Dalyellioida, typhloplanoida: Byrsophlebidae und trigonostomidae. *Fauna Fenn.* **12**, 1–71 (1962).

27. J. A. Goodheart, A. E. Bely, Sequestration of nematocysts by divergent cnidarian predators: Mechanism, function, and evolution. *Invertebr. Biol.* **136**, 75–91 (2017).

28. E. M. J. Laetz, H. Wägele, Chloroplast digestion and the development of functional kleptoplasty in juvenile *Elysia timida* (Risso, 1818) as compared to short-term and non-chloroplast-retaining sacoglossan slugs. *PLOS ONE* **12**, e0182910 (2017).

29. G. Christa, V. Zimorski, C. Woehle, A. G. M. Tielens, H. Wägele, W. F. Martin, S. B. Gould, Plastid-bearing sea slugs fix CO_2 in the light but do not require photosynthesis to survive. *Proc. Biol. Sci.* **281**, 20132493 (2013).

30. G. Christa, K. Händeler, P. Kück, M. Vleugels, J. Franken, D. Karmeinski, H. Wägele, Phylogenetic evidence for multiple independent origins of functional kleptoplasty in Sacoglossa (Heterobranchia, Gastropoda). *Org. Divers. Evol.* **15**, 23–36 (2015).

31. E. R. Schockaert, Turbellarians, in *Methods for the Examination of Organismal Diversity in Soils and Sediments*, G. S. Hall, Ed. (CAB International, 1996), pp. 211–225.

32. M. Kearse, R. Moir, A. Wilson, S. Stones-Havas, M. Cheung, S. Sturrock, S. Buxton, A. Cooper, S. Markowitz, C. Duran, T. Thierer, B. Ashton, P. Meintjes, A. Drummond, Geneious basic: An integrated and extendable desktop software platform for the organization and analysis of sequence data. *Bioinformatics* **28**, 1647–1649 (2012).

33. S. Picelli, O. R. Faridani, Å. K. Björklund, G. Winberg, S. Sagasser, R. Sandberg, Full-length RNA-seq from single cells using Smart-seq2. *Nat. Protoc.* **9**, 171–181 (2014).

34. M. G. Grabherr, B. J. Haas, M. Yassour, J. Z. Levin, D. A. Thompson, I. Amit, X. Adiconis, L. Fan, R. Raychowdhury, Q. Zeng, Z. Chen, E. Mauceli, N. Hacohen, A. Gnirke, N. Rhind, F. di Palma, B. W. Birren, C. Nusbaum, K. Lindblad-Toh, N. Friedman, A. Regev, Full-length transcriptome assembly from RNA-Seq data without a reference genome. *Nat. Biotechnol.* **29**, 644–652 (2011).

35. B. J. Haas, A. Papanicolaou, M. Yassour, M. Grabherr, P. D. Blood, J. Bowden, M. B. Couger, D. Eccles, B. Li, M. Lieber, M. D. MacManes, M. Ott, J. Orvis, N. Pochet, F. Strozzi, N. Weeks, R. Westerman, T. William, C. N. Dewey, R. Henschel, R. D. LeDuc, N. Friedman, A. Regev, De novo transcript sequence reconstruction from RNA-seq using the Trinity platform for reference generation and analysis. *Nat. Protoc.* **8**, 1494–1512 (2013).

36. D. R. Laetsch, M. L. Blaxter, BlobTools: Interrogation of genome assemblies. *F1000Res.* **6**, 1287 (2017).

37. D. R. Laetsch, G. Koutsovoulos, T. Booth, J. Stajich, S. Kumar, DRL/blobtools: BlobTools v1.0.1 (2017); doi:10.5281/ZENODO.845347.

38. H. Gruber-Vodicka, E. Pruesse, B. K. B. Seah, phyloFlash (2017); https://github.com/HRGV/phyloFlash.

39. F. A. Simão, R. M. Waterhouse, P. Ioannidis, E. V. Kriventseva, E. M. Zdobnov, BUSCO: Assessing genome assembly and annotation completeness with single-copy orthologs. *Bioinformatics* **31**, 3210–3212 (2015).

40. R. M. Waterhouse, M. Seppey, F. A. Simão, M. Manni, P. Ioannidis, G. Klioutchnikov, E. V. Kriventseva, E. M. Zdobnov, BUSCO applications from quality assessments to gene prediction and phylogenomics. *Mol. Biol. Evol.* **35**, 543–548 (2018).

41. C. E. Laumer, A. Hejnol, G. Giribet, Nuclear genomic signals of the 'microturbellarian' roots of platyhelminth evolutionary innovation. *eLife* **4**, e05503 (2015).

42. D. M. Bryant, K. Johnson, T. DiTommaso, T. Tickle, M. B. Couger, D. Payzin-Dogru, T. J. Lee, N. D. Leigh, T.-H. Kuo, F. G. Davis, J. Bateman, S. Bryant, A. R. Guzikowski, S. L. Tsai, S. Coyne, W. W. Ye, R. M. Freeman Jr., L. Peshkin, C. J. Tabin, A. Regev, B. J. Haas, J. L. Whited, A tissue-mapped axolotl de novo transcriptome enables identification of limb regeneration factors. *Cell Rep.* **18**, 762–776 (2017).

43. K. Katoh, H. Toh, Improved accuracy of multiple ncRNA alignment by incorporating structural information into a MAFFT-based framework. *BMC Bioinformatics* **9**, 212 (2008).

44. R. Lanfear, B. Calcott, S. Y. W. Ho, S. Guindon, PartitionFinder: Combined selection of partitioning schemes and substitution models for phylogenetic analyses. *Mol. Biol. Evol.* **29**, 1695–1701 (2012).

45. A. Stamatakis, RAxML version 8: A tool for phylogenetic analysis and post-analysis of large phylogenies. *Bioinformatics* **30**, 1312–1313 (2014).

46. F. Ronquist, J. P. Huelsenbeck, MrBayes 3: Bayesian phylogenetic inference under mixed models. *Bioinformatics* **19**, 1572–1574 (2003).

47. J. P. Huelsenbeck, B. Rannala, Frequentist properties of Bayesian posterior probabilities of phylogenetic trees under simple and complex substitution models. *Syst. Biol.* **53**, 904–913 (2004).

48. S. E. Hamsher, K. M. Evans, D. G. Mann, A. Poulíčková, G. W. Saunders, Barcoding diatoms: Exploring alternatives to COI-5P. *Protist* **162**, 405–422 (2011).

49. J. H. Levialdi Ghiron, thesis, Università degli Studi di Messina, Messina, Italy (2006).

Citation: N. W. L. Van Steenkiste, I. Stephenson, M. Herranz, F. Husnik, P. J. Keeling, B. S. Leander, A new case of kleptoplasty in animals: Marine flatworms steal functional plastids from diatoms. *Sci. Adv.* **5**, eaaw4337 (2019).